PREDICTING RESPONSE TIMES OF FIXED-TEMPERATURE, RATE-OF-RISE, AND RATE-COMPENSATED HEAT DETECTORS BY UTILIZING THERMAL RESPONSE TIME INDEX OF DETECTORS

Soonil Nam
FM Global, 1151 Boston-Providence Turnpike, Norwood, MA 02062

ABSTRACT

A project was initiated to find a way of assigning thermal response time index (RTI) of heat detectors and to see if a detector response time could be estimated by utilizing the assigned RTI value. In Phase 1 of the project, the concept was applied to fixed temperature rating detectors and estimating detector response times were successfully implemented. In the second part of the project, rate-of-rise detectors and rate-compensated detectors were investigated. Test data employing a plunge-tunnel of varying air temperatures were used to extract RTI values of a rate-of-rise detector and rate-compensated detectors. In the final stage of the project, adequacy of estimating detector response times of rate-of-rise and rate-compensated detectors based on RTI values in conjunction of other threshold values for activation was assessed. Twenty-seven real-scale fire tests were conducted to see if the estimated response times match well with the measured detector response times. Test results showed that the detector response time estimation based on RTI values matched well with the measured ones. Having the ability of predicting detector response times in association of fire scenarios provides a great flexibility in deploying heat detectors in filed operations. Detectors can be installed at performance based spacing with respect to detector types and anticipated fire growth scenarios. Bench-scale tests to assign RTI values of detectors can replace the real-scale fire tests for the maximum spacing that are costly while less than reliable. Detector response sensitivity can be classified by the value of RTI and the maximum spacing of a detector can be assigned based on its RTI value.

1. INTRODUCTION

As heat detectors are not only being used as a warning device but also widely used as a trip device of automatic fire suppression systems, it is increasingly desirable for a fire safety engineer to have a reliable means of predicting heat detector activation times if a fire growth rate can be prescribed. Early work[1] established this goal by assigning Response Time Index (RTI) to each fixed-temperature-rating heat detector utilizing a plunge-tunnel[1, 2].

The types of heat detectors that were not covered in the work[1] were detectors activated by <u>rate of rise</u> of temperatures and <u>rate-compensated</u> detectors. A study was carried out in order to find a way to find detector response times in connection with RTI values of those detectors. Five different models of detectors were chosen for plunge tunnel tests. In the plunge tunnel, the air temperatures were varied with different rates of rise. Methods to extract the response time index from plunge tunnel test data were developed. Then the methods were validated by comparisons of the estimated response times based

on the assigned RTI values with measured response times in real-scale fire tests. In order for readers to be able to follow the text without frequent pauses, and also to make this paper to be a stand-alone one, portions of the early work[1] and data were re-introduced in this paper.

Three types of heat detectors have been investigated in the overall program: fixed temperature rating, rate-of-rise, and rate-compensated detectors. Thermal sensitivities of the detectors were measured through bench-scale tests using plunge-type wind-tunnels that provided an air flow of a fixed velocity with either a fixed temperature or temperatures increasing at a fixed rate. Five restorable and four non-restorable models of the fixed-temperature rating type were the subjects of the early study[1]. One restorable model of rate-of-rise type, and four restorable models of rate-compensated type detectors were used in the current study. A small number of test samples per each model were subjected to plunge-tunnel tests. In general, each test sample was exposed up to 10 plunge-tunnel tests determining the thermal sensitivity of the sample in order to reduce the influence associated with possible measurement variations. Then a response time index (RTI) value was obtained for each model of the detectors by averaging the measured RTI values of the test samples belonging to the same model.

The detector models used in the program are given in Table 1. The temperature ratings (the 2nd column) in the table are the ones assigned by listing organizations after they were verified through the oven tests[3]. The rate-of-rise detectors do not have a temperature rating; thus, the value in the temperature rating column corresponding to Rate-of-Rise Model RR-A detector is the threshold value of rate-of-rise of temperature in ^{o}C/s for the activation of the detector. The third column shows whether a detector is restorable or not. All the fixed-temperature rating detectors in Table 1, Model FTR-A through FTR-K, were investigated in Ref 1; thus, they will not be discussed in detail here. The rate-of-rise detector and the rate-compensated detectors will be discussed in detail and some applications will be proposed based on the study.

2. THEORY

If one can assume that detectors are activated by convective heat transferred through the fire plume, the energy balance equation on the heat sensing element of the detector can be given as

$$mc\frac{dT_e}{dt} = hA(T_g - T_e) \tag{1},$$

where m is the mass of the heat sensing element, c is the specific heat of the element, T_e is the sensing-element temperature, t is time, h is the convective heat transfer coefficient, A is the sensing-element surface area, and T_g is the surrounding hot air temperature.   By

introducing the time constant $\tau \equiv \frac{mc}{hA}$ [2] and $\tau = RTI \big/ \sqrt{u}$ [2], Eq 1 can be transformed to

$$\frac{dT_e}{dt} = \frac{T_g - T_e}{\tau} = \frac{\sqrt{u}}{RTI}\left(T_g - T_e\right) \tag{2}.$$

2

TABLE 1: TEST DETECTOR MODELS

Detector Model ID	Temperature Rating (°C)	Restorable/ Non- Restorable	Reference
Fixed Temp. Rating Model **FTR-A**	57	Restorable	Type A in Ref 1
Fixed Temp. Rating Model **FTR-B**	77	Restorable	Type B in Ref 1
Fixed Temp. Rating Model **FTR-C**	57	Restorable	Type C in Ref 1
Fixed Temp. Rating Model **FTR-D**	93	Restorable	Type D in Ref 1
Fixed Temp. Rating Model **FTR-E**	88	Restorable	Type E in Ref 1
Fixed Temp. Rating Model **FTR-H**	57	Non-Restorable	Type H in Ref 1
Fixed Temp. Rating Model **FTR-I**	90	Non-Restorable	Type I in Ref 1
Fixed Temp. Rating Model **FTR-J**	57	Non-Restorable	Type J in Ref 1
Fixed Temp. Rating Model **FTR-K**	93	Non-Restorable	Type K in Ref 1
Rate-of-Rise Model **RR-A**	0.139 (°C/s)	Restorable	Current Study
Rate-Compensated Model **RC-B**	57	Restorable	Current Study
Rate-Compensated Model **RC-C**	57	Restorable	Current Study
Rate-Compensated Model **RC-D**	71	Restorable	Current Study (Type F in Ref 1)
Rate-Compensated Model **RC-E**	88	Restorable	Current Study (Type G in Ref 1)

Here *RTI* is the Response Time Index of a detector that indicates a thermal response sensitivity of the sensing element to the surrounding hot gas (mostly air) originated by a fire plume, and u is the flow velocity at the detector. The *RTI* can be measured through the plunge tunnel tests[1, 2]. Once the response time index (*RTI*) of a heat detector is known, detector response times can be computed by obtaining T_e vs. t through the integration of Eq 2. T_g and u in the equation either can be estimated by fire scenarios or measured through fire tests.

If the air temperature increases at a fixed rate inside a plunge-tunnel, then the temperature of the flowing air flow will become,

$$T_g = Kt + T_{g0} \tag{3},$$

where K is the rate of rise of temperature, t is time, and T_{g0} is the initial gas temperature. By defining $x \equiv T_g - T_e$, Eq 2 can be converted to

$$\frac{dx}{dt} = \frac{dT_g}{dt} - \frac{dT_e}{dt}$$
$$= K - \frac{dT_e}{dt} \qquad (4).$$

By combining Eqs 2 and 4,

$$\frac{dT_e}{dt} = K - \frac{dx}{dt}$$
$$= \frac{x}{\tau} \qquad (5).$$

Integrating Eq 5 yields

$$T_e = T_g - K\tau - (T_{g0} - T_{e0} - K\tau)\exp(-t/\tau) \qquad (6),$$

where T_{e0} is the initial detector sensor temperature. Eq 6 shows that

$$\frac{dT_e}{dt} = K\left(1 - e^{-t/\tau}\right) + \frac{(T_{g0} - T_{e0})}{\tau}e^{-t/\tau} \qquad (7).$$

For the convenience of measuring τ, the last term in Eq 7 can be deleted by having the test sample exposed to surrounding gas flow for a long enough time before a test starts, thus, making $T_{g0}=T_{e0}$. Then, Eq 7 for activation of a rate-of-rise detector can be solved as

$$C_r = K\left(1 - e^{-t/\tau}\right) \qquad (8),$$

where C_r is the threshold rate of rise of temperature that would activate the detector.

Then

$$\tau = \frac{-t_f^i}{\ln\left(1 - \frac{C_r}{K}\right)} \qquad (9),$$

where t_f^i is the elapsed time from the beginning of temperature rise to activation of the detector at the plunge tunnel. Once τ is known, the response time index (RTI) can be computed[2] by

$$RTI = \tau\sqrt{u} \qquad (10),$$

where u is the constant air flow velocity inside the plunge tunnel during the test.
A fixed-temperature rating detector activates when T_e becomes the temperature rating, T_r.
A rate-of-rise detector activates when

$$\left(T_g - T_e\right)\big/\tau \geq C_r \qquad (11).$$

A rate-compensated detector activates when T_e becomes the virtual temperature rating, T_{rv}, which will be discussed shortly.

3. ASSIGNING RTI VALUES TO VARIOUS DETECTOR TYPES BASED ON THE BENCH-SCALE TEST DATA

3.1 Fixed temperature rating detectors

The RTI of a fixed-temperature rating heat detector (Model FTR-A through Model FTR-K in Table 1) was measured by plunging the detector samples into a tunnel, in which an air flow has a fixed temperature and velocity, until the test samples activated[1]. Eq 2 was numerically integrated with the known T_g (197 ^{o}C) and u (1.55 m/s) and found the *RTI* value that made T_e become the temperature rating, T_r, at the measured activation time. For each restorable-detector model, five samples were chosen and ten tests were conducted for each sample. Then the average value of the 50 data points was assigned as the *RTI* value of the given model[1]. Fig 1 shows one such example.
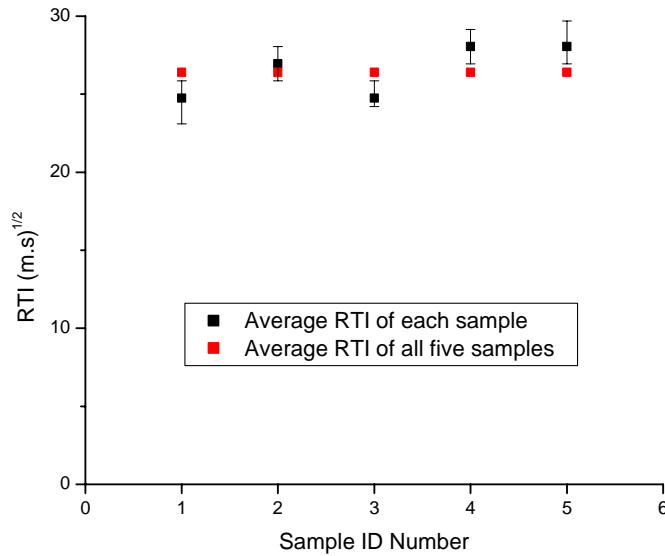
Fig 1. Average RTI value of fixed-temperature-rating type detector samples FTRC1-C5.

3.2 Rate-of-rise type detectors

Among the five models of the test samples used in the current study, only one detector model, RR-A, was found to be activated solely by the rate of rise of temperature. A total of 34 plunge tunnel tests were conducted at 3 different rates (K) with four test samples. The average air velocities used in the tests were varied from 1.53 m/s to 2.2 m/s. Fig 2 shows the air temperature variation with respect to time during a test. The test sample was inside the tunnel for 446 s before the air temperature inside the plunge tunnel started to increase. Note that the numbers in the abscissa of the figure correspond to 0.1 second intervals. During the period of the first 446 s, the ambient temperature inside the tunnel was well maintained at a flat temperature so that it would not affect the test outcome. Also the time was long enough to treat the initial sensor temperature as the same as the ambient air temperature inside the tunnel.

As the air temperature started to rise at t_i=446 s, and the detector sample activated at t_f=578 s, a temperature variation between that period had to be analyzed in detail. The

temperature at t_i was 22.4 °C and that at t_f was 48.9 °C, which were denoted as T_i and T_f in the following equations, respectively.

The rate of rise K can be found as

$$K = \frac{T_f - T_i}{t_f - t_i} = \frac{48.9 - 22.4}{578 - 446} = 0.201 \quad (^oC/s) \tag{12}.$$
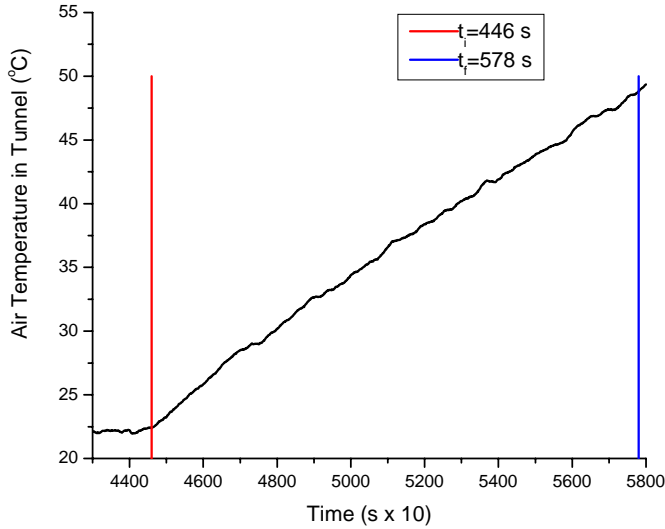
Fig 2. Air temperatures inside the plunge tunnel between t_i and t_f.

The average air flow velocity between t_i and t_f measured by a Pitot tube came out as 1.53 m/s. Now τ can be calculated by Eq 9. Once τ is determined after finding a proper C_r, RTI can be obtained by RTI=$\tau\sqrt{u}$. Although the listed C_r value was 0.139 °C/s (15 °F/min), no independent measurement data on C_r were available. Thus, a way to find the true C_r value of the tested samples had to be devised. FM Approvals conducts tests for a rate of rise detector inside an oven[3], in which temperature of air flow increases at the rate of 0.185 °C/s until the detector sample activates. It is, therefore, reasonable to assume that the C_r value must be less than 0.185 °C/s. RTI values associated with the tested samples were computed using Eq 9 with the C_r varied between 0.12 °C/s and 0.18 °C/s with an increment of 0.01 °C/s in conjunction with the measured plunge-tunnel test data. It is reasonable to assume that the C_r value corresponding to the smallest standard deviation of RTI values would be the closest to the real C_r value that the tested detector samples had. The analysis based on the collected data indicated that Cr=0.15 provides the minimum standard deviation; thus, C_r=0.15 °C/s was chosen for Model RR-A detectors. With C_r=0.15 °C/s, Eq 9 provides the value of τ and eventually RTI values.

3.3 Rate-compensated heat detectors

Detector Models RC-B, RC-C, RC-D, and RC-E in Table 1 were all identified by screening tests, which will be discussed later, as rate-compensated detectors. Fig 3 shows

6

the air temperatures inside the tunnel at activation of the tested samples vs. various initial air temperatures. The figure indicates that each detector model activates, more or less, at a fixed air temperature regardless of the differences in the initial air temperatures. Fig 4 shows the air temperatures at activation of test samples vs. various K's used in the tests. The figure indicates that each detector model activates at a fixed air temperature regardless of the differences in the rate-of-rise of the air temperatures (K) adopted in the tests. Figs 3 and 4 clearly show that the <u>test samples activate at the temperatures far below the listed temperature ratings</u> of each detector model, which were obtained through the standard oven tests[3] at listing organizations. The average air temperature at activation of each model in Fig 3, which must be higher than the temperature at the detector sensing element, was 50 ^{o}C for Model RC-B, 47 ^{o}C for Model RC-C, 62 ^{o}C for Model RC-D, and 74 ^{o}C for Model RC-E, while the corresponding temperature ratings in Table 1 are substantially higher. The plunge-tunnel test results shown in Figs 3 and 4 strongly suggest that the test samples behave as if they were fixed temperature rating detectors; however, their true temperature ratings, which are denoted as *virtual temperature ratings, T_{rv}*, would be lower than the corresponding listed temperature ratings.
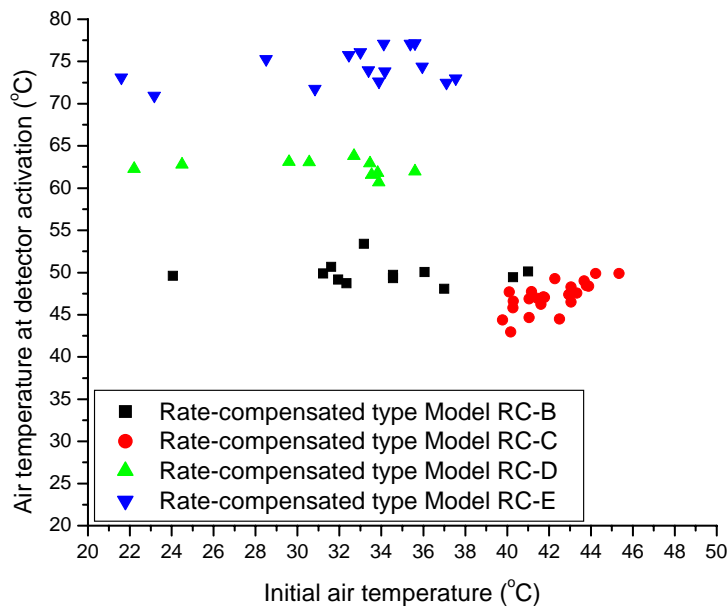
Fig 3. Initial air temperature inside the plunge-tunnel vs. the air temperature at detector activation.

As the RTI value and the virtual temperature rating of each model detector had yet to be determined, the data collected with the plunge-tunnel with the variable air temperature alone were not sufficient to extract both *RTI* and T_{rv}. Thus, more data were collected with the plunge-tunnel with a fixed temperature. Then potential RTI values corresponding to possible T_{rv} values were computed. The numerical integration of Eq 2 was used to extract *RTI* and T_{rv} values from the data collected with the fixed temperature plunge-tunnel, while Eq 4 was used for the data collected with the varied temperature plunge-tunnel.
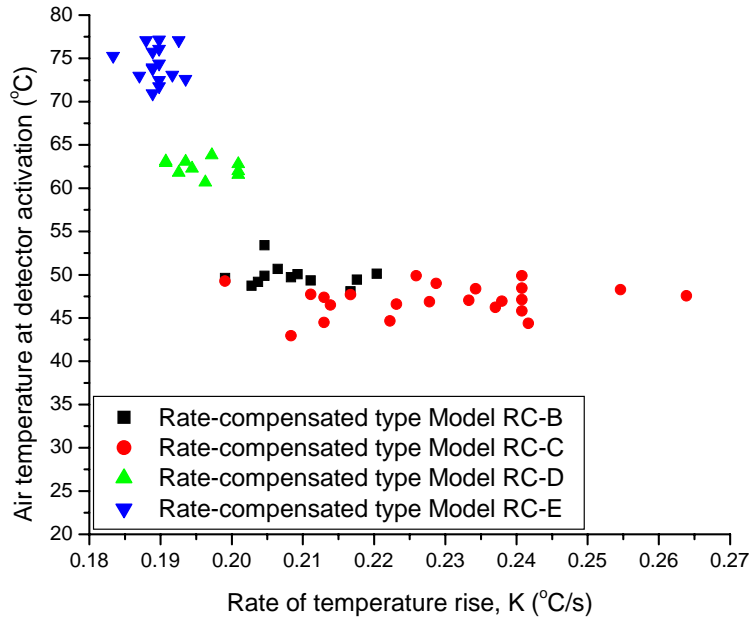
Fig 4. Rate of rise of air temperature inside the plunge-tunnel (K) vs. air temperature at detector activation.

As the virtual temperature rating of a RC detector is not known *in priori*, the RTI values from fixed temperature plunge tunnel test data cannot be computed directly. Thus, a range of possible temperature rating had to be guessed and the RTI values corresponding to each possible temperature rating were to be assessed. Using the possible RTI values obtained above, possible range of T_{rv} were then calculated by utilizing the data obtained in plunge-tunnel tests conducted with varying air temperatures. To do so, Eq 6 has been utilized. When T_e in Eq 6 becomes T_{rv}, the detector activates, and T_{g0}-T_{e0} becomes zero if the test samples are exposed to the ambient tunnel temperature for a long-enough period prior to the increase of tunnel air temperature. For the t and K in the equation, the Activation time and Rate of Rise, respectively, should be used. The τ in the equation can be obtained by $\tau = RTI/\sqrt{u}$. The RTI and T_{rv} values are given in Table 2.

TABLE 2: *RTI* AND T_{rv} VALUES OF RATE-COMPENSATED TYPE DETECTORS

Detector Test Samples	*RTI* $(m.s)^{1/2}$	Virtual Temperature Rating, T_{rv} (^{o}C)	Listed Temperature Rating, Tr (^{o}C)
Model RC-B	5.5	49.1	57
Model RC-C	8.5	48.3	57
Model RC-D	33.1	57.5	71
Model RC-E	32.1	71.4	88

For the sake of completion, the RTI and T_r values of the other detector samples used in the study are given in Table 3.

<u>TABLE 3: RTI AND T_v OR C_r VALUES OF FIXED-TEMPERATURE RATING AND RATE-OF-RISE TYPE DETECTORS</u>

Detector Test Samples	RTI $(m.s)^{1/2}$	Listed Temperature Rating (^{o}C)
Fixed Temp. Rating Model FTR-A	65.1	57
Fixed Temp. Rating Model FTR-B	69.0	77
Fixed Temp. Rating Model FTR-C	14.4	57
Fixed Temp. Rating Model FTR-D	12.7	93
Fixed Temp. Rating Model FTR-E	8.8	88
Rate-of-Rise Model RR-A	156	C_r=0.15 (^{o} C/s)

4. COMPARISONS OF ESTIMATED WITH MEASURED RESPONSE TIMES

In order to see if the concept and the processes employed to obtain the RTI values of the detectors described in Section 3 are valid, detector response times estimated based on the obtained RTI values were compared with the response times actually measured in fire tests. A total of 27 tests were conducted under the movable ceiling of Research Laboratory at FM Global Research Campus, West Glocester, Rhode Islands, USA. The following is a brief description of fire tests.

4.1 Fire Tests Configuration

Ten detector samples (two samples per each model of RR and RC's), two velocity probes, and two sprinklers were installed on the ceiling along the circumference of a 3.4-m radius circle in the east-west direction. The fire source was to be located at the center of the circle. As shown in Fig 5, the detector samples were installed in the following order from the east- to the west-direction: Sprinkler 1, Detector RR-A1, Detector RC-B1, Detector RC-C1, Velocity Probe 1, Detector RC-D1, Detector RC-E1, Sprinkler 2, Detector RR-A2, Detector RC-B2, Detector RC-C2, Velocity Probe 2, Detector RC-D2, and Detector RC-E2.

The dimension of the room where the tests were conducted was 30 m (east-west) by 42 m (north-south) by 9 m high.   The dimension of the movable ceiling was 24 m by 12 m. The ceiling heights were varied few times in the test program. The location of the fire source, which was the origin of the 3.4 m radius circle, was 7.5 m from the south wall and 5.7 m from the north wall. The distance between each detector/velocity probe/sprinkler sample was maintained at 0.15 m edge to edge. When detector response times were estimated, the temperatures and velocities measured at Velocity Probe 1 were used for Detector RR-A1 through Detector RC-E1, and those at Velocity Probe 2 were used for Detector RR-A2 through Detector RC-E2. Note that although the sprinklers were installed as reference detectors, estimating sprinkler response times were not pursued as the information provided for the sprinkler characteristics were deemed unreliable.   It was also learned after Test 17 that the direction of the installed Detector

RC-C1 and RC-C2 were 90 degree off from the direction used in the plunge-tunnel tests. Thus, all the data associated with Model RC-C detectors in Test 1 to Test 17 were deleted. Additional ten fire tests were carried out after Model RC-C detector samples were installed properly.

Detector activation times were estimated by using the *RTI* and T_{rv} (or C_r in the cases of RR-A1 and RR-A2) of each detector model, which are shown in Table 2. The detector response times were found by numerically integrating T_e in Eq 2 with the measured values of u and T_g in fire tests. When, $\left(T_g - T_e\right)\big/\tau$ becomes greater than C_r, Detector sample RR-A1 and RR-A2 will activate. For all the other detector samples, a detector will activate when T_e becomes greater than T_{rv} of the detector.
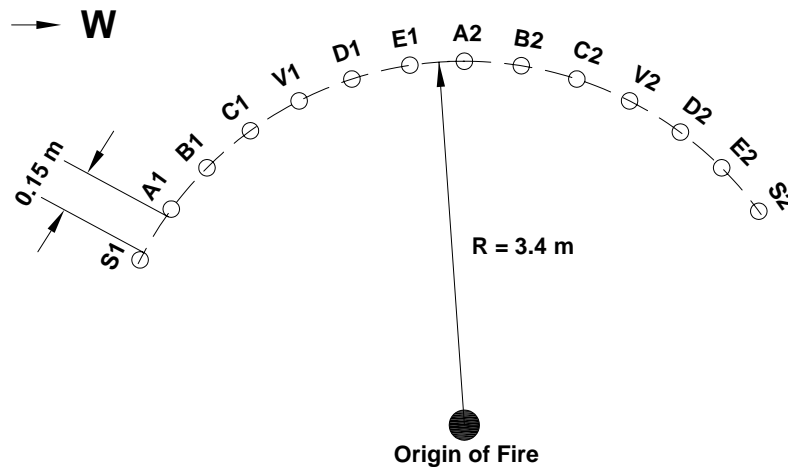
Fig 5. Schematic of the test sample locations.   They were placed a 0.15 m-edge-to-edge distance between the samples. Here S1 and S2 denote Sprinklers 1 and 2; V1 and V2 denote Velocity Probes 1 and 2; and A1 through E2 correspond to, respectively, Detector RR-A1 through Detector RC-E2.

4.2 Test Fires

The test fire was a heptane spray fire for Tests 1 through 9, Tests 13 through 17, and Test 22 through 27. The flow rate of heptane was designed to be 15 GPH, which would generate an approximately 480 kW fire, while the fuel pump was designed to maintain a 100 psi pressure for the duration of the test. Fig 6 shows a typical spay fire that was used in the test program. The test fires for the other tests were wood-crib fires, one of which is shown in Fig 7. The expected maximum heat release rate from each crib was approximately 300 kW.

Fig 6. Heptane spray fire used in tests. Test detector samples can be seen in the right.

Fig 7. One of the crib fires used in the test program.   Depending on the test, one or two cribs were used.

4.3 Overall Comparisons of the Estimated and the Measured Response Times per Each   Detector Model

The estimated detector response times based on the *RTI* and T_{rv} (or C_r) of test detector samples in conjunction with the measured air temperatures and velocities at detector sample locations in each test were compared with the measured ones in the real tests. Fig 8 shows the cases with the rate-of-rise detectors, Model RR-A. The estimated response times match well with the measured ones. The comparisons for the cases with slow growing fires, such as crib fires used in the test program, look more favorable than those in the tests with spray fires, which reached their maximum heat release rates with almost no inception periods.
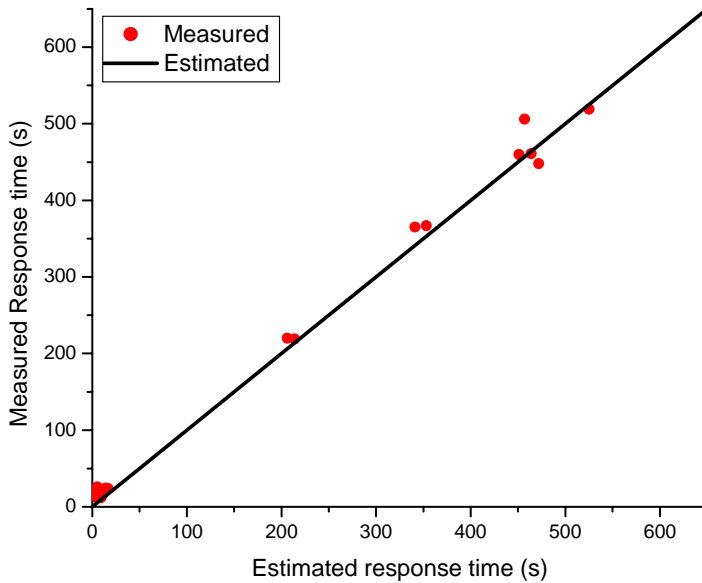
Fig 8. Comparison of the measured and the estimated response times of <u>rate-of- rise</u> heat-detector samples of the same model

Fig 9 shows the ambient air temperatures at activation of RC-B detectors in fire tests. They all look random and would not be possible to predict when the detector will activate just based on the air temperature at activation alone.   Fig 10 shows the air temperature at activation vs. the average rate-of-rise of air temperature for RC-B detectors in fire tests. Here the average rate of rise of air temperature ($\overline{K}$) was calculated as (Air temperature at activation-Initial air temperature in a fire test)/activation time. The figure does not reveal any specific trend of activation temperatures with respect to the average rate of rise of temperatures. Similar behaviors of the air temperatures at activation were observed in cases with the other detectors too. Again, predicting detector activation just based on the air temperature at activation alone would not be possible. However, when the *RTI* and T_{rv} of Detector RC-B were utilized, the prediction came out quite good as shown in Fig 11.
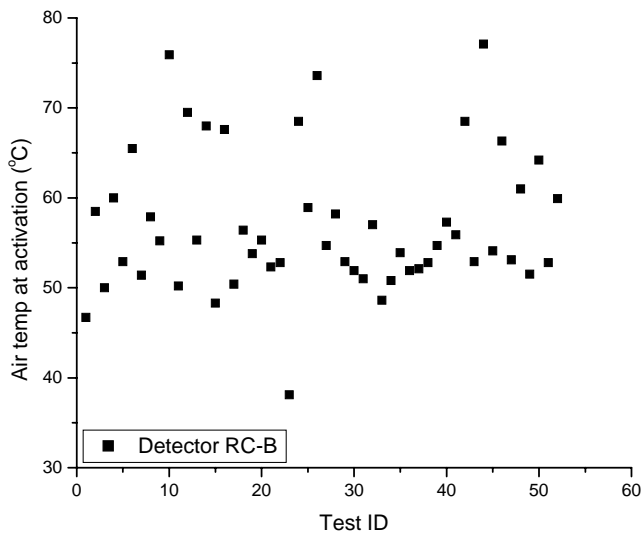
Fig 9. Air temperature at activation of RC-B detector samples in fire tests.
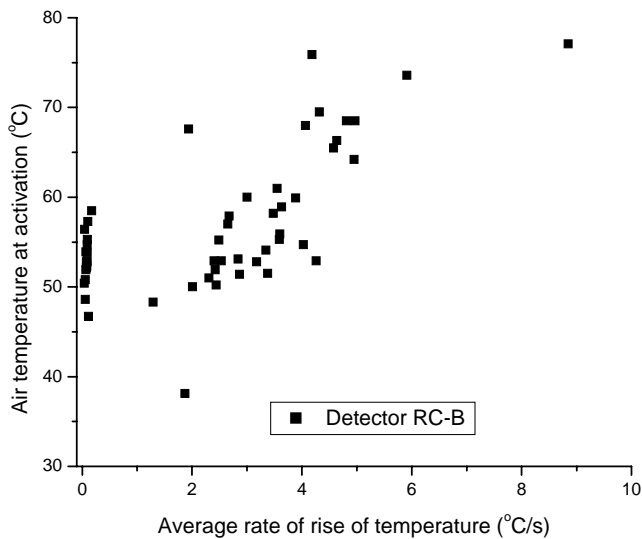
Fig 10. Air temperature at activation vs. $\overline{K}$ of RC-B detector samples in fire tests.

Fig 12 shows the test results of the cases with RC-C, RC-D, and RC-E detectors. The results with RC-B were also included for a comparison. The figure shows that the predicted respond times match reasonably well with the measured ones for Model RC-C detectors. Note that the comparison of the measured and estimated response times for Model RC-C detector samples are only in fire tests 18 through 27. The figure indicates that the match in tests using spray fires are more favorable than those in the tests using crib fires for Model RC-C detectors. The degrees of discrepancies in the fire tests using crib fires, slow growing fires, are greater than that in the tests with the spray fires.
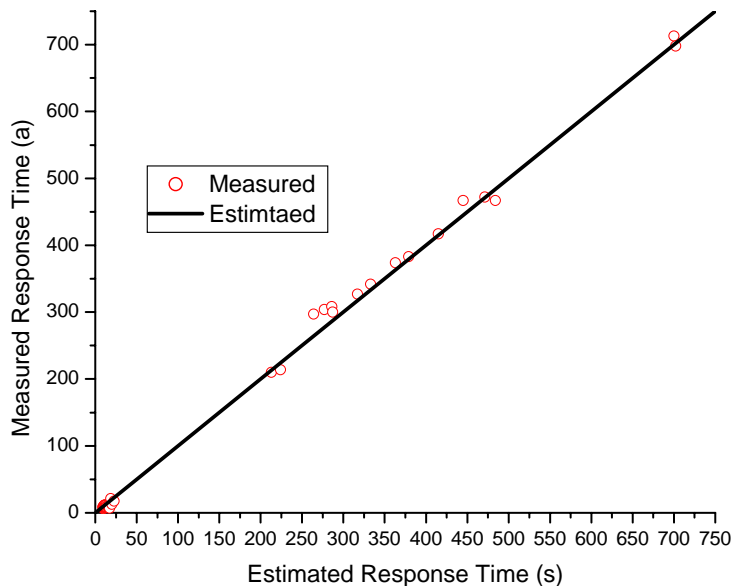
Fig 11. The measured vs. the estimated response times of RC-B detectors in fire tests.

For RC-D detector samples, the estimated response times are within an acceptable range of the measured ones for practical applications. The figure shows that the matches are excellent when detector response times are generally short, i.e., under fast growing fires, but less accurate when the response times are long, i.e., under slow growing fires. For the tests with Model RC-E detectors, except for a few cases of poor matches, the estimated response times match well with the measured ones. It was noticed that when Model RC-E detector samples were exposed to repeated fire tests, they sometimes either took a considerably longer times before to respond than normally expected, or did not respond at all. There was a possibility that if the tests were conducted with a much slower phase, thus provided longer pauses between the tests, the detector samples might have responded differently.

Overall, the body of test results indicate that predicting detector response times using the model developed in the current study works reasonably well. The relatively large deviations associated with rate-compensated type detector Models D and E in Fig 12 are related to the cases where the test fire sizes with respect to the detector locations were marginal to activate the detectors in the first place.   Also the heat release rates of the test fires already had peaked at some point before the end of the test; thus, prolongation of the test did not significantly contribute to the increase of temperature and velocity of air surrounding the detector samples. In those cases, instead of a comparison of response times, a comparison of estimated and measured fire sizes at activation could have been a better indicator of the precision of the prediction. In all the other cases, where the fire sizes were not marginal for detector activation or fires grew continuously, as expected in most field operations, the comparisons of the response times show good matches.

14
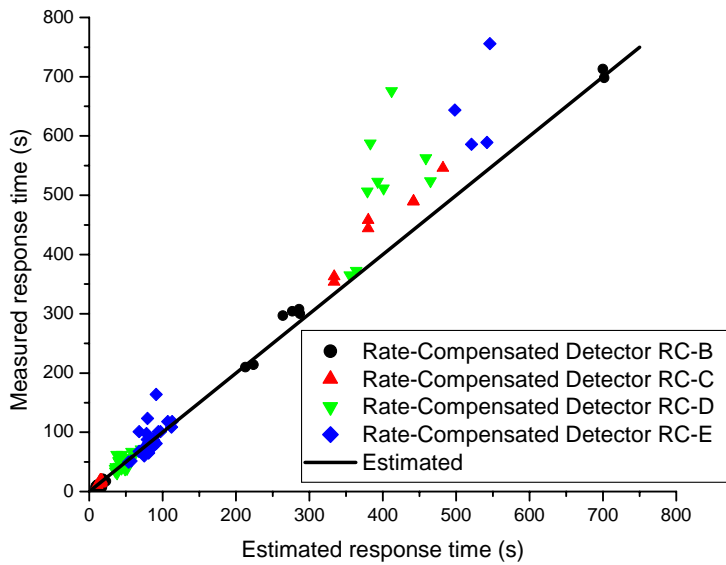
Fig 12. Comparison of the measured and the estimated response times of rate-compensated heat- detector samples from four different models.

For the purpose of completion, comparisons of the measured and the estimated response times of fixed-temperature-rating detector samples in fire tests from the early work[1] are given in Fig 13.
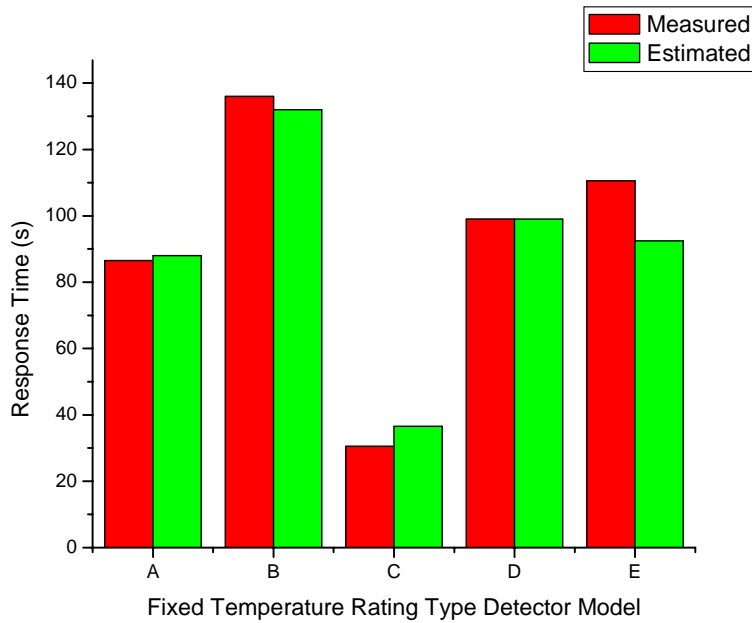
Fig 13. Comparison of the measured and the estimated response times of fixed-temperature-rating heat detectors.

In summary, the concept of predicting detector response times by using the response time index of heat detectors and the methodology of assigning the RTI values through bench-scale tests seem to be acceptable. The capability of predicting response times will provide larger flexibility to fire safety engineers in choosing detector types and assigning the maximum detector spacing than currently being practiced.

5. OTHER APPLICATIONS OF BENCH-SCALE TESTS TO HEAT DETECTORS

5.1 Bench-Scale Tests in Classification of Detector Types

Plunge-tunnel tests with varied air temperature were useful for classifying whether certain detectors were a rate-of-rise type or a rate-compensated type. Simple tests revealed that one of the most widely circulated rate-of-rise detectors was in fact not a rate-of-rise type detector. Figs 14 and 15 show how one can identify a rate-of-rise detector from other detector types. Fig 14 shows that the air temperatures at detector activation of a rate-of-rise detector linearly increase with the initial air temperatures while that of a rate-compensated detector show no clear dependence on the initial air temperatures. Fig 15 shows that while the detector activation times of a rate-of-rise detector are relatively constant regardless of the initial air temperatures, those of a rate-compensated detector are inversely proportional to the initial air temperatures. During the tests in Figs 14 and 15, K was maintained at 0.2 ^{o}C/s.
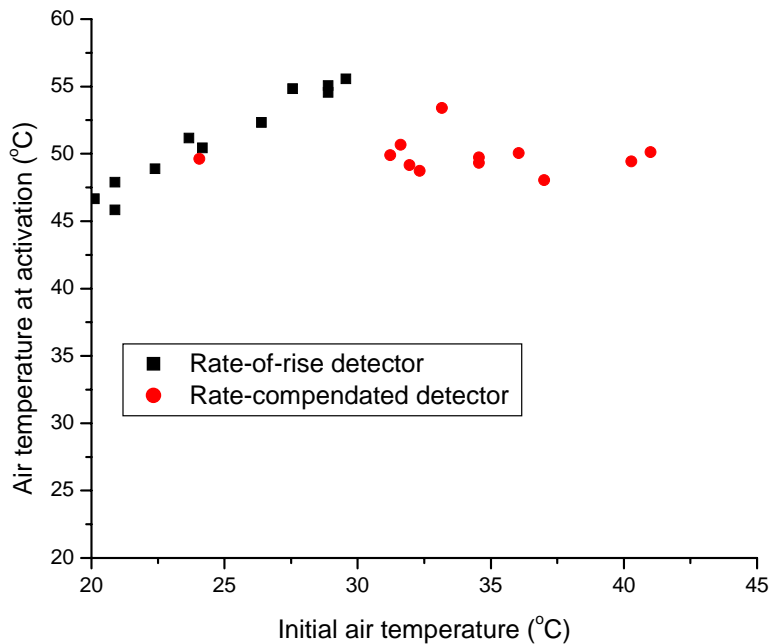
Fig 14. Initial air temperature inside the plunge-tunnel vs. the air temperature at detector activation (K=0.2 ^{o}C/s).
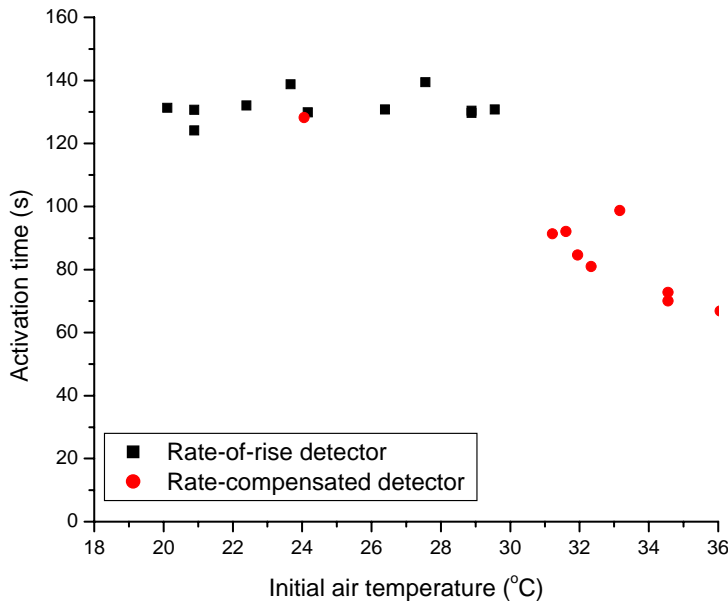
Fig 15. Initial air temperature inside the plunge-tunnel vs. detector activation time (K=0.2 ^{o}C/s).

5.2 Bench-Scale Test Application for Product Quality Control

It is important that manufactured detectors maintain a reliable quality control so that the end users can expect consistent performance under similar circumstances. However, there is no reliable test method or enforced standard to guarantee this. The bench-scale tests utilizing a plunge-tunnel similar to the one used in this study can be used as a good screening tool to measure a degree of the quality control of products. Fig 16 shows the RTI values obtained through the data utilizing a fixed-temperature plunge-tunnel. The test samples were two different models of fixed-temperature-rating non-restorable types, FTR-I and FTR-H. Twenty samples per each model were used in the tests. Based on Fig 16, one can deduct that Model FTR-I would provide more consistent performance than Model FTR-H might. A listing organization can suggest an acceptable tolerance in the quality of products and verify the tolerance through bench-scale tests.

6. APPLICATION OF THE RTI CONCEPT TO FIELD OPERATIONS

Currently, heat detectors are approved through two sets of tests: Oven tests and real-scale fire-tests[3]. The oven tests verify the posted temperature rating of heat detectors while real-scale fire tests are employed to determine the maximum spacing that is to be assigned to detectors. The RTI values obtained through the bench-scale tests can be used to assign the maximum spacing of a detector without going through real-scale fire tests. Assigning the maximum spacing based on the RTI value has the following advantages over the current method: (1) It has been known that determining the maximum spacing

17
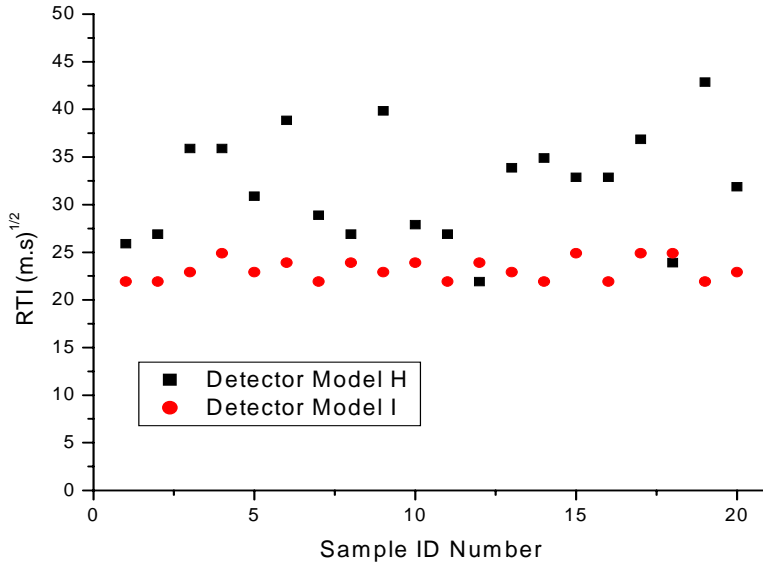
Fig 16. RTI values of non-restorable fixed temperature rating detector Model H and I.

based on real-scale fire tests is not as reliable as it should be. Depending on a device that is adopted for the reference detector (a sprinkler is commonly used), the size of a standard test fire, the size of room where tests are conducted, or an ambient temperature while tests are conducted, the tests can provide wide range of different results for an identical type of detectors. Many detectors that are listed for a 15.2-m spacing by UL end up with a 7.6-m spacing at FM Approvals despite similar test protocols. This inconsistency is not limited to inter-testing organizations. Even at the same testing site, the same detector can be assigned to different spacing values if tests are conducted with two ambient temperatures that are widely different from each other. The spacing values based on RTI values of detectors will eliminate these inconsistencies. (2) Replacing real-scale fire tests with bench-scale tests will reduce the costs associated with detector approvals. (3) Detector spacing can be flexibly adjusted to meet custom-tailed specific demands.

A practical guide to the use of the RTI concept for detectors can be illustrated through demonstrations of predicting detector response times under various fire scenarios. Once RTI and T_{rv} (or C_r for the rate-of-rise detectors) are known, the response can be predicted with a known fire scenario. The following examples will show how the detector spacing can be achieved:

Detector response times with respect to threshold fire sizes were estimated by utilizing RTI and T_{rv} (or T_r or C_r) of ten detector models in Table 1. The temperature rating (T_r) of the detectors in Ref 1 are given in Table 1 and the RTI values are: 65.1, 69.0, 14.4, 12.7, and 8.8 in $(m.s)^{1/2}$, respectively from FTR-A through FTR-E[1]. The RTI values and T_{rv} (or C_r) values of the detector used in the current work are given in Table 5. The detector response time of each detector was calculated with the following three different spacing values---3.0 m by 3.0 m, 9.1 m by 9.1 m, and 15.2 m by 15.2 m. The fire growth rate was

assumed the same as that of the medium growing fire of NFPA 72[4]. The following will show how detector response times at different spacing values can be estimated.

The fire scenario described in NFPA 72 as the medium growing fire has the following heat release rate:

$$\dot{Q}_T = 0.0117t^2 \tag{13},$$

where $\dot{Q}_T$ is the total heat release rate from a fire in kW and t is the time after ignition in second. To stay in a conservative side, it can be assumed that the fire source is directly below the center of the specified maximum detector spacing, which is the most remote location from the detectors.

The plume correlations can be given as follows[5]:

$$\Delta T_0 = C_{\Delta T_0} \left[(T_\infty) \Big/ (g C_p^2 \rho_\infty^2) \right]^{1/3} \dot{Q}_c^{2/3} (z - z_0)^{-5/3} \tag{14},$$

$$V_{z0} = C_{V_{z0}} \left[(g) \Big/ (C_p \rho_\infty T_\infty) \right]^{1/3} \dot{Q}_c^{1/3} (z - z_0)^{-1/3} \tag{15},$$

where ΔT_0 is the excess temperature at the plume centerline (K), T_∞ is the ambient temperature (K), g is the gravitational acceleration (m/s^2), C_p is the constant pressure specific heat of air (kJ/kg K), ρ_∞ is the density of ambient air (kg/m^3), $\dot{Q}_c$ is the convective heat release rates (kW) calculated as $\eta_c \dot{Q}_T$ (here η_c is the convective portion of HRR and chosen as 0.65) , z is the elevation from the source of the plume (m), and z$_0$ is the virtual origin of the plume (m). The plume coefficient for temperature, $C_{\Delta T_0}$, was taken as 9.1 and $C_{V_{z0}} = 3.1$[5]. It is assumed that the ambient temperature is 20 $^\circ$C, virtual origin z$_0$ is close to zero, and the detectors are mounted on a 9.1-m high ceiling, which is the ceiling height of many warehouses.

The ceiling mounted detectors are located at 2.16-m, 6.47-m, and 10.78-m radial distance from the fire plume axis. In order to estimate the fire plume velocities and the temperatures at the detector locations, the correlations that show the velocities and the temperatures as a function of a radial distance r from a plume centerline axis need to be known, preferably in functional forms. The ceiling jet flow correlations in Ref 6 are used here. The correlation of the ceiling jet temperatures in Ref 6 is

$$y = y_0 + \left[a \Big/ (w\sqrt{\pi/2}) \right] \exp\left\{ -2\left[(x - x_c) \Big/ w \right]^2 \right\} \tag{16},$$

where $y \equiv \log(\Delta T / \Delta T_0)$, y_0=-0.00781, a=-1.2788, w=1.23898, $x \equiv \log(r/b)$, and x_c=1.51005. Here $\Delta T(r)$ is the excess ceiling flow temperature at location r, normalized by ΔT_0, which is the excess temperature of an unobstructed fire plume axis at the elevation corresponding to a ceiling height h. The radial distance, r, was normalized by

b, which is a plume half-width of an unobstructed fire plume at the elevation corresponding to the ceiling height h. The plume half width can be calculated by[5],

$$b = 0.12 \left(T_0 \Big/ T_\infty \right)^{1/2} (z - z_0) \tag{17},$$

where T_0 is $\Delta T_0 + T_\infty$. Ref 6 also shows a collection of data showing $V_r \Big/ V_{z0}$ vs. (r/b). V_r is the radial directional flow velocity at r and V_{z0} is the centerline axial velocity of an unobstructed fire plume at the elevation corresponding to a ceiling height h. The correlation curve given in the figure is the same as Eq. (16), however, with different values of the parameters. Here $y \equiv \log(V_r / V_{z0})$, y_0=-0.05514, a=-0.79891, w=0.79131, and x_c=1.31777.

The temperature and velocity variations with time at r=2.16 m, r=6.47 m, and r=10.78 m can be obtained by applying Eqs 14 through 17. Then Eq 2 can be numerically integrated until T_e reaches the virtual detector temperature rating, T_{rv}, in Table 2 for rate-compensated detectors (or $dT_e \Big/ dt \geq C_r$ in the case of rate-of-rise detectors) or T_r in Table 1 for fixed-temperature-rating detectors. Table 4 shows the response times of the detectors at the three spacing locations. The fire growth was simulated for 30 min. When the computation showed that a detector would activate, then the response time and the HRR at the activation are given.

TABLE 4. DETECTOR RESPONSE TIMES IN THE GIVEN FIRE SCENARIO

Detector Model ID	R1 (3.0 m by 3.0 m)		R2 (9.1 m by 9.1 m)		R3 (15.2 m by 15.2 m)	
	$t_{activation}$ (s)	$\dot{Q}_T$ (kW)	$t_{activation}$ (s)	$\dot{Q}_T$ (kW)	$t_{activation}$ (s)	$\dot{Q}_T$ (kW)
RR-A	282	929	759	6750	1316	20307
RC-B	254	754	395	1829	522	3189
RC-C	250	734	389	1777	514	3099
RC-D	319	1192	486	2772	637	4754
RC-E	395	1830	597	4172	777	7067
FTR-A	332	1294	500	2935	653	5000
FTR-B	441	2283	657	5059	851	8482
FTR-C	306	1100	471	2602	619	4485
FTR-D	495	2874	740	6411	956	10709
FTR-E	469	2579	704	5807	912	9742

As shown in Table 4, once RTI values of all models of detectors are assigned, then detector response times can be estimated under a given fire scenario. Instead of assigning the maximum spacing blindly based on certain standard fire tests, the maximum spacing of detectors can be estimated based on custom tailored fire scenarios and an acceptable maximum fire size at detector activation. The ability of predicting detector response times in association of fire sizes provides a means of site specific, thereby more efficient, use of detectors. The practice above illustrates the flexibility that is lacking in a rigid prescription of maximum spacing values that come with the current detector spacing. A

field engineer can evaluate the most appropriate detector and its spacing based on an anticipated fire growth scenario and response requirements at a given site with the current method. The detector also can be linked to a fire suppression system as a reliable trip device as an engineer can predict when the detector will activate under a prescribed environment.

Ref 6 shows how the maximum spacing of a fixed-temperature-rating detector can be assigned when the detector works as a device tripping a pre-action valve in a dry-pipe system. The example in the reference shows that by having the ability of predicting the detector response time, it was possible to assign the maximum detector spacing without compromising the full benefit of having the pre-action valve in the given dry-pipe sprinkler system. There can be more similar examples of performance based spacing once all detectors are approved with their known RTI values, rather than the current practice of assigning the maximum spacing value of a detector that has a limited value in practical applications. In case a listing organization wants to maintain the current way of assigning the maximum spacing values that are linked to activation of a certain reference device, it can be achieved in a similar way described above. By computing response times of the reference device using its own RTI and T_r values under the given fire scenario, one can decide the maximum spacing values of a detector by comparing the response times of the detector at few radial locations with that of the reference device at the specified location.

If there is a desire by industry, heat detectors can be classified based on the response sensitivity. One possible scenario is that heat detector sensitivities are classified as standard response, fast response, and ultra-fast response, similar to the current classification of sprinklers. A range of RTI values can be assigned to each classification.

7. SUMMARY AND CONCLUSIONS

Three subjects covered in this paper are: obtaining RTI values of rate-of-rise and rate-compensated heat detectors through bench-scale tests, validating through real-scale fire tests the methodology of assigning RTI values, and applying the RTI concept to product approvals and field operations.
Detector samples from five different models---one rate-of-rise and four rate-compensated detector types---were exposed to plunge-tunnel tests to measure response times where hot air was circulated with the temperature varying at a fixed rate. The RTI and C_r (threshold rate-of-rise for activation) of the rate-of-rise detector, Model RR-A, were obtained by analyzing the test data.

However, rate-compensated detectors needed more plunge-tunnel tests. Plunge-tunnel test data indicated that rate-compensated detectors behave as if they were fixed-temperature-rating detectors albeit that their true temperature rating values (virtual temperature rating) would be substantially lower than their corresponding listed temperature rating values. Finding the RTI and the virtual temperature rating values of rate-compensated detectors (T_{rv}) required additional sets of plunge-tunnel test data. One more set of tests were conducted with the tunnel that provided the air flow of a fixed

temperature.   Possible combinations of *RTI* and T_{rv} values obtained from the two sets of test data were plotted to find a common value. The intersection point of the average *RTI* and T_{rv} values estimated from two sets of data was chosen for the *RTI* and the virtual T_{rv} values of the rate-compensated detectors.

Once the *RTI* and T_{rv} (or C_r) values were obtained, the validity of the concept and the methodology were tested through 27 real-scale fire tests. Ten detector samples, two each from the five models, were installed on a movable ceiling and exposed to either heptane spray fires or crib fires.   Detector response times were recorded together with the temperatures and velocities of the ceiling jet flows at detector locations. The estimated detector response times that were calculated by utilizing the *RTI* and T_{rv} (or C_r) values of the detector samples in conjunction of measured temperatures and velocities of the fire plumes were compared with the measured ones. The comparisons were favorable and thus provided confidence in the methodology and the concept.

The ability of predicting detector response times by utilizing the RTI values that would be obtained through bench-scale tests will provide a great flexibility for field operations in choosing detector types and maximum spacing values of a chosen detector.   A heat detector can be a reliable tripping device of a fire suppression system as one can predict the fire size at the tripping time. The real-scale fire tests that are currently being used as the standard tests by listing organizations to assign the maximum spacing value of a detector, which are costly while less than reliable, can be completely eliminated as the spacing values can be easily determined by computations utilizing the *RTI* and T_{rv} (or C_r, or T_r) value of the detector.   Some examples were provided how this can be achieved.

REFERENCES

1. Soonil Nam, Leo P. Donovan, and Jieon Grace Kim, "Establishing Heat Detectors' Thermal Sensitivity Index through Bench-Scale Tests," *Fire Safety Journal,* vol. 39, 2004, pp. 191-215.
2. Heskestad, G. and Smith, H. F., "Investigation of a New Sprinkler Sensitivity Approval Test: The Plunge Test," Technical Report, FMRC J. I. 22485, Factory Mutual Research Corporation, 1151 Boston-Providence Turnpike, Norwood, Massachusetts, 1976.
3. "Thermostats for Automatic Fire Detection," Class Number 3210, FM Approvals, 1151 Boston-Providence Turnpike, Norwood, Massachusetts, 1978.
4. NFPA 72, *National Fire Alarm Code*, 2002 Edition. National Fire Protection Association, 1 Batterymarch Park, Quincy, Massachusetts.
5. Heskestad, G, "Engineering relations for fire plumes," *Fire Safety J.*, vol. 7, 1984, pp. 25-32.
6. Soonil Nam, **"**A Case Study: Determination of Maximum Spacing of Heat Detectors**,"** *Journal of Fire Protection Engineering*, vol 15, pp. 5-18, 2005.